power ratios at high incidence, it is recommended that precalculated or tested propeller data for the zero angle-of-incidence values be used. If calculated or test thrust and power data is unavailable, use can be made of the zero incidence thrust and power equations presented. Comparison with experiment shows an engineering accuracy sufficient for establishing design criteria, trending studies, and preliminary configuration development, and performance estimates. All these results are applicable for propellers operating at high incidence or in large upflow and are thus applicable to VTOL-type operation as well as for conventional propeller operation.

### References

[1] Ribner, H. S., "Formulas for propellers in yaw and charts of the side-force derivative," NACA Rept. 819 (1943).

[2] Ribner, H. S., "Propellers in yaw," NACA Rept. 820 (1943).

[3] Ribner, H. S., "Notes on the propeller and slip stream in relation to stability," NACA ARR L4I12a (WR L-25).

[4] Yaggy, P. F. and Rogallo, V. L., "A wind tunnel investigation of three propellers through an angle-of-attack range from 0° to 85°," NASA TN D-318 (May 1960).

[5] Von Mises, R., *Theory of Flight* (Dover Publications, Inc., New York, 1959), Chap. XI, pp. 302–309.

[6] Gessow, A. and Myers, G. P., *Aerodynamics of the Helicopter* (The Macmillan Co., New York, 1952), Chap. 8, p. 190.

[7] Fung, Y. C., *The Theory of Aeroelasticity* (John Wiley and Sons, Inc., New York, 1955), Chap. 6, p. 216.

[8] *Aeroelasticity Symposium, Gottingen, April 16–17, 1957*, NASA TT F-81, p. 45 (September 1963).

[9] Bland, S. R. and Bennett, R. M., "Wind-tunnel measurement of propeller whirl-flutter speeds and static-stability derivatives and comparison with theory," NASA TN D-1807 (August 1963).

[10] De Young, J., "Force and moment derivatives due to propellers of arbitrary configuration inclined with respect to freestream," AIAA Preprint 64-169 (1964).

MAY-JUNE 1965 J. AIRCRAFT VOL. 2, NO. 3

# An Application of Hydropneumatic Propulsion to Hydrofoil Craft

JOHN D. PIERSON*
*Martin Company, Baltimore, Md.*

**The design of large, high-speed hydrofoil craft is dependent upon the development of reliable and efficient means of converting very high power levels to effective thrust. A novel means has been developed which uses compressed air directly to produce thrust in an underwater, ramjet-like cycle: the MARJET hydrofoil, an integrated lifting propulsive system. The theory of operation is briefly reviewed, and the practical problems of incomplete mixing and heat transfer are discussed. Experimental data are presented to confirm the analysis and provide correlation factors for design use. Basic design charts for the internal performance of the MARJET and the related foil drag are presented, along with a recommended procedure for optimization of an integrated MARJET-hydrofoil design. A sample application to a large 80-knot hydrofoil craft shows that performance competitive with that forecast for supercavitating propellers would require multistage air compression with intercooling to approach isothermal conditions. However, used as a booster system, the MARJET will provide flexible and efficient high-speed thrust augmentation even with conventional turbocompressors for the air supply.**

## Introduction

THE design of large, high-speed hydrofoil craft requires a practical means of converting high power levels to thrust efficiently. Gas turbines can provide the necessary power at reasonable installed weight, but structural and arrangement problems make the conversion of the shaft power to thrust a real challenge to the designer. Developments in supercavitating propellers, high-speed gearing, pumps, and associated systems are extending the range of thrust production, but further growth in this direction may be limited by poor service life at high stress levels.

A propulsion system that uses compressed air as the power transmission medium, with direct conversion to thrust in a hydrodynamic ramjet, has been under development at the Martin Company for several years. Called MARJET, this system is inherently rugged and capable of large power conversion in vehicles moving through the water at high speed. Although MARJET may be pertinent to many fields of marine propulsion, the most recent development work has been directed toward its application to high-speed hydrofoil craft with the support of the Machinery Design Branch, Bureau of Ships.[1, 2]

An artist's concept of a MARJET-hydrofoil design is shown in Fig. 1. The basic powerplant (contained within the hull) consists of several engine-compressor units. The air from the compressors may be ducted together and distributed to the several foils through air passages within the struts and foils. The flexibility in design and the simplicity of the air power distribution and control are the prime advantages of the MARJET system.[1, 4] The question that remains, how well the air power can be converted to thrust, is the subject of this paper.

The combined MARJET hydrofoil is an integrated lifting propulsive system. The MARJET is incorporated within the lifting surface by splitting the normal foil shape and separating upper and lower surfaces to form the internal duct

Presented as Preprint 64-305 at the 1st AIAA Annual Meeting, Washington, D. C., June 29–July 2, 1964; revision received November 23, 1964. Work supported by Machinery Design Branch, Bureau of Ships.

* Senior Staff Engineer.

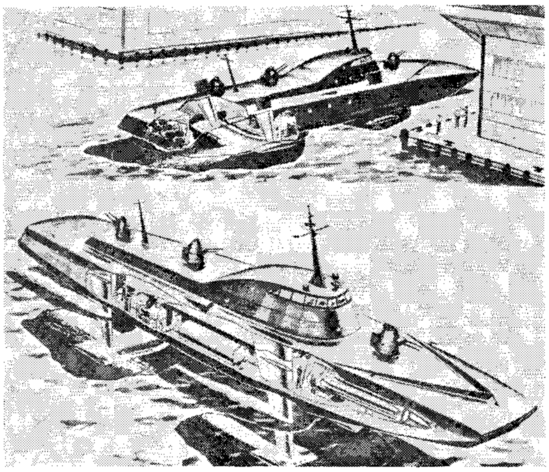

**Fig. 1 MARJET hydrofoil.**

as shown in Fig. 2. The basic effect of the MARJET is to develop thrust by a change in momentum of the enclosed stream of water by the direct work of expansion of air within the water.

## MARJET Cycle Analysis

The MARJET (Fig. 2) is essentially 1) an inlet and diffuser to convert total stream pressure to a higher static pressure by reducing the velocity, 2) an injection area at the end of the diffuser to introduce air into the water stream, 3) a mixing area and expansion nozzle to develop the work of expansion of the air in the water, 4) a faired external shape from inlet to exit, and 5) an air supply source.

In reports on early development tests[3] and in feasibility studies,[1] the analysis of the MARJET cycle was based upon ideal conditions of uniform mixing of the air and water. Although such ideal performance is not actually achieved, the corresponding analytical relationships provide a basis for performance evaluation. Two equations may be written for the ideal MARJET:

Continuity

$$AV = Q_w + (2120/P)^{1/\gamma} Q_A \qquad (1)$$

Momentum

$$dP = -\rho_M V\, dV \qquad (2)$$

where

$A$ = cross-sectional area (span × height)
$V$ = velocity
$Q_w$ = water flow rate
$Q_A$ = air flow rate (standard conditions $P$ = 2120)
$P$ = static pressure
$\rho_M$ = mass density of flow (adiabatic flow neglecting mass of air)
$\rho_M = \rho/[1 + (2120/P)^{1/\gamma} Q_A/Q_w]$
$\rho$ = mass density of water

In the diffuser section $Q_A$ is zero, and the typical relation for total head is

$$P_T = P + (\rho/2)V^2 = P_{T_0} - P_D = P_0 + (\rho/2)V_0^2 - P_D \qquad (3)$$

where

$$\begin{aligned} P_T &= \text{total head} \\ (\ )_0 &= \text{freestream conditions} \\ P_D &= \text{head loss in inlet and diffuser} \\ q_0 &= (\rho/2)V_0^2 = P - P_0 + P_D + (\rho/2)V^2 \end{aligned} \qquad (4)$$

The effect of the air injection and expansion is an increase in the total head of the water flow as indicated by the integration of Eq. (2) downstream from station 2:

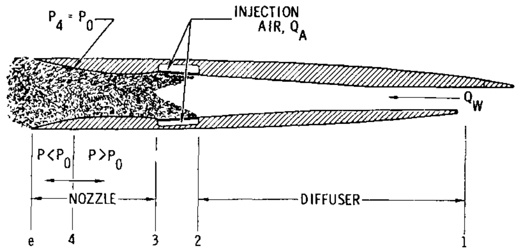


**Fig. 2 Basic MARJET components, typical section.**

$$\int_{P_2}^{P} \frac{dP}{\rho_M} = \int_{P_2}^{P} \left[1 + \left(\frac{2120}{P}\right)^{1/\gamma} \frac{Q_A}{Q_w}\right] \frac{dP}{\rho} =$$
$$-\int_{V_2}^{V} V dV - \frac{Q_A}{Q_w} \int_{P_2}^{P} \left(\frac{2120}{P}\right)^{1/\gamma} dP = P_T - P_{T_2} \qquad (5)$$

The internal thrust of the MARJET is arbitrarily defined as the change in momentum between the approaching freestream and the conditions at station 4 where the static pressure returns to the ambient value. (In practically all of the cases the actual exit for the MARJET hydrofoil will have a greater area and lower pressure as indicated in Fig. 2. Although the velocity and momentum would continue to increase past station 4, the base pressure overcomes the gain in thrust. This base drag is treated separately as such.)

For internal thrust (where air mass flow is negligible),

$$F = \rho Q_w (V_4 - V_0) \qquad (6)$$

The velocity ratio $V_4/V_0$ is obtained from Eqs. (3–5):

$$\frac{V_4}{V_0} = \left[1 - \frac{P_D}{q_0} - \frac{1}{q_0}\frac{Q_A}{Q_w}\int_{P_2}^{P_4} \left(\frac{2120}{P}\right)^{1/\gamma} dP\right]^{1/2} \qquad (7)$$

On the basis of test data from MARJET models with air supplied at various temperatures,[2] it has been concluded that the air expansion is isothermal at the water temperature. Thus, the ideal work integral can be evaluated

$$-\frac{1}{q_0}\frac{Q_A}{Q_w}\int_{P_2}^{P_4=P_0=2120} \left(\frac{2120}{P}\right) dP = \frac{Q_A}{Q_w}\frac{2120}{q_0} \ln \frac{P_2}{2120} \qquad (8)$$

and the MARJET internal thrust, in nondimensional form, is

$$\frac{FV_0}{q_0 Q_A} = 2\frac{Q_w}{Q_A}\left[\left(1 - \frac{P_D}{q_0} + \frac{Q_A}{Q_w}\frac{2120}{q_0}\ln\frac{P_2}{2120}\right)^{1/2} - 1\right] \qquad (9)$$

The ideal cycle performance is plotted in Fig. 3. The work output $FV_0$ and the work input (isothermal) 2120 $Q_A$ ln($P_2$/2120) are made nondimensional by dividing by the product of the freestream dynamic head $q_0$ and the air flow rate $Q_A$. The major parameter is the air-to-water flow ratio $Q_A/Q_w$. The curves shown have been calculated from Eq. (9) with the

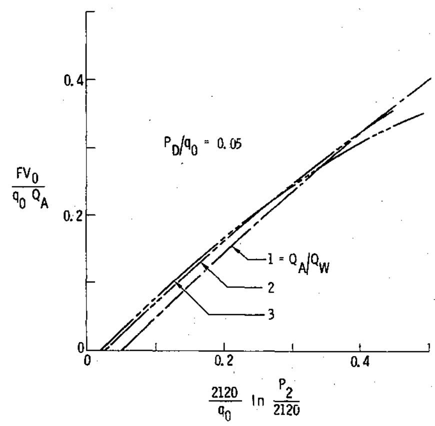


**Fig. 3 MARJET performance, ideal cycle.**

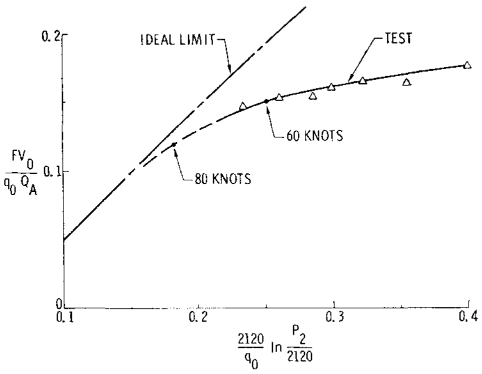


**Fig. 4 Typical test comparison with ideal.**

assumption of 5% loss for the inlet and diffuser $P_D/q_0 = 0.05$. (This loss is consistent with development test data from a specific MARJET model[3] as well as general hydrodynamic data for diffuser design.)

## Experimental Data

The ideal performance of the MARJET cycle analysis depends upon the complete and uniform mixing of the air and water. The extent to which such conditions could be attained has been the subject of a number of research and development test programs. The most recent tests[2] have formed the basis for design data charts for full-scale size and speeds to 80 knots.

A typical plot of model test results is compared with the ideal performance in Fig. 4 for an air-to-water ratio of 2. The difference between the curves represents the losses due to incomplete mixing and unequal velocity distribution across the sections. These physical phenomena, which might be deduced from the performance data, were confirmed by direct observation of the flow with the aid of Fastax motion pictures and exit plane traverse measurement of flow rate and total pressure. With increasing air-water ratio, the mix becomes progressively poorer and more air escapes along the nozzle boundaries. However, with increasing speed, the mixing itself is noticeably improved, and the performance tends toward the ideal limit.

The major physical parameter for the MARJET performance is the ratio of the nozzle throat area $A_*$ to the area at the beginning of injection $A_2$. In combination with the air-to-water ratio $Q_A/Q_w$ and the forward speed $V_0$, the area ratio $A_*/A_2$ determines the performance. The basic model test program[2] consisted of 29 configurations with variations in size, proportions, and injection details. Although minor variations in performance were noted among these many configurations, only the $A_*/A_2$ ratio showed a consistent and controlling influence on the MARJET internal performance. Figure 5 shows the generalized plot of the internal performance for MARJET at 60- and 80-knot speeds. This generalized plot represents the composite of the large number of individual data curves such as that shown in Fig. 4.

Comparison of the test-based plots with the ideal mix lines in Fig. 5 shows the extent to which MARJET actually produces thrust with respect to its cycle potential based upon isothermal expansion. (The isothermal basis is used since a number of model tests with hot air supply showed no increase in performance over cold air supply and since the measured exhaust characteristics compared closely with calculations based upon isothermal conditions.)

The efficiency for any point in the parameter plot is the slope of the line joining the point with the origin (air assumed supplied at water temperature)

$$\eta = \frac{FV_0/q_0Q_A}{(2120/q_0)\ \ln(P_2/2120)} = \frac{FV_0}{2120Q_A\ \ln P_2/2120} = \frac{\text{output work}}{\text{input work}}$$

This efficiency is related to the internal performance of the MARJET at zero draft with isothermal input power. In actual practice, the MARJET hydrofoil must operate at a substantial draft (to allow for rough water operation), and the air may be supplied at high temperature. These conditions will reduce the MARJET system performance. Also, some portions of the external drag should be charged to the MARJET performance.

## Effect of Draft

The primary effect of draft is the increase in ambient pressure. From the viewpoint of the MARJET internal performance, the change in pressure and volume conditions of the flow is inconsequential with respect to the existing pressures in high-speed operation. However, the atmospheric air supply must be compressed to a greater extent to supply the increase in pressure due to the draft. As indicated in Fig. 6, the ratio of the usable work input ($P_2$ to $P_0$) as compared to the isothermal compressor input ($P_2$ to 2120) is

$$\eta_{\text{draft}} = (\ln P_2/P_0)/\ln(P_2/2120)$$

where

$$P_0 = 2120 + \rho g(\text{draft, ft})$$

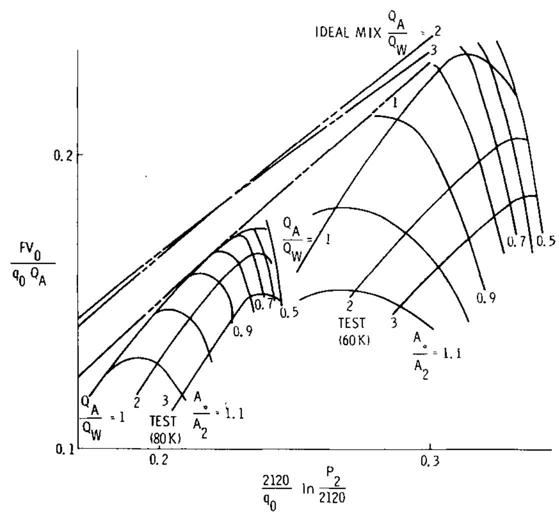


**Fig. 5 MARJET basic performance chart.**

## Air Supply System

The efficiency of air compressors is usually based upon their performance with respect to ideal adiabatic compression

$$\eta_{\text{compression}} = \frac{2120Q_A3.5[(P/2120)^{1/3.5}-1]}{\text{shaft work input}} \cong 0.85$$

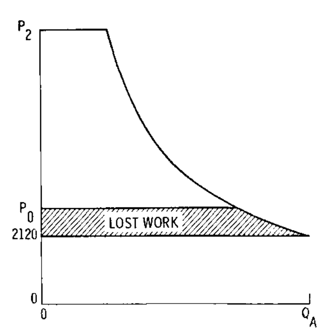


**Fig. 6 Effect of draft on input power.**

However, the MARJET does not utilize the work represented by the heat of compression (see Fig. 7). If hot air is supplied, it is rapidly cooled to the water temperature at injection, and the expansion process is substantially isothermal. From this view the air supply efficiency is

$$\eta_{\text{air supply}} = \frac{2120 Q_A \ln P/2120}{\text{shaft work input}}$$

For the simple air compressor (no interstage cooling), this yields a basic cycle efficiency limitation

$$\eta_{\text{cycle}(0)} = \frac{\ln P/2120}{3.5[(P/2120)^{1/3.5} - 1]}$$

and

$$\eta_{\text{air supply (0)}} = 0.85\eta_{\text{cycle (0)}}$$

For two-stage compression (one intercooler) the lost work is considerably reduced

$$\eta_{\text{cycle}(1)} = \frac{\ln P/2120}{7[(P/2120)^{1/7} - 1]}$$

With many compression stages and corresponding intercoolers, it would be theoretically possible to approach isothermal compression. However, construction requirements, pressure losses in the intercoolers, and similar practical problems would limit the feasibility of such multistage air compression systems in high power applications.

## External Drag

Several external drag factors are affected by MARJET and must be considered in the determination of the net thrust of the MARJET hydrofoil: skin friction, profile drag, and base drag. These depend upon the combined geometry of the internal duct, suitable structure, and external shape consistent with the desired operating speed range.

In most cases the planform area of foil required for lift will be sufficient to contain the MARJET required for thrust. Thus the foil skin friction will be the same as for other methods of propulsion and need not be evaluated for comparison or optimization studies.

The profile drag has a definite relation to the MARJET, since the thickness of the over-all foil must be sufficient to contain the required MARJET flow areas. In particular, the area at the beginning of injection $A_2$ is determined by the total water flow $Q_w$ and the geometric area ratio $A_*/A_2$. The area $A_2$ for a given water flow increases as the area ratio $A_*/A_2$ decreases. The corresponding increase in foil thickness yields increase in profile drag.

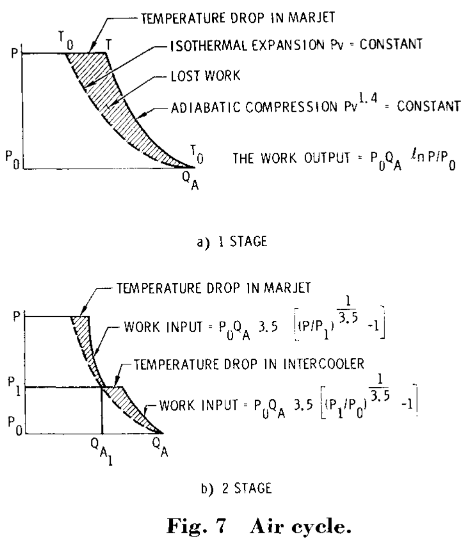


**Fig. 7 Air cycle.**

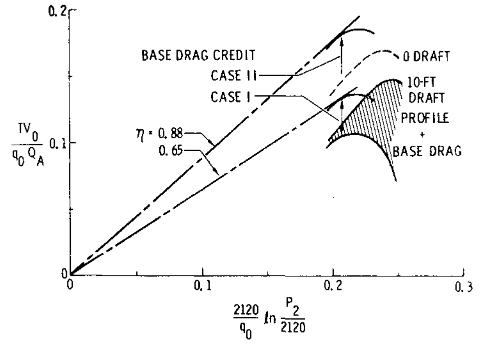


**Fig. 8 Typical net MARJET performance (10-ft draft, 80 knots, 5% inlet and diffuser loss).**

The total base area of a MARJET hydrofoil is much greater than the base of a plain hydrofoil providing lift only. This does not necessarily lead to a high base drag, because the MARJET exhaust fills the base area. The amount of base drag depends upon how nearly the base area matches the requirement for the area of ambient exhaust pressure $A_4$. As mentioned previously, the internal thrust is arbitrarily defined as the resultant momentum change up to station 4. Beyond this point the pressure continues to drop as the section gets larger. The below-ambient pressure acting on the area increase from $A_4$ to $A_e$ (see Fig. 2) causes the base drag. The drop in pressure may be limited to the pressure in the external flow field, but in any case the base drag is high for large exit area (small $A_*/A_2$, large $A_2$). The typical effect of the external drag (profile and base) on the net MARJET performance is shown in Fig. 8.

## Design Application

The thrust of MARJET depends upon the development of high static pressure in the injection area. This pressure is obtained by recovery of the dynamic water pressure in the diffuser. For this reason the characteristic thrust of a MARJET is zero at rest and increases with speed as shown in Fig. 9. Generally, propellers and jet pumps have an opposite characteristic. The resistance vs speed for a typical hydrofoil craft lies between these characteristics: a rapid rise to the hump at minimum foil speed is followed by a drop-off in resistance to the best flying speed, and then the foil-borne resistance increases again with further increase in speed.

If MARJET is to be used as the primary propulsion at high speed, a low-speed boost (propeller or pump) will be required. A typical composite curve representing this system is shown in Fig. 9 (curve $A$). When propellers or pumps provide the primary power, the effect of assigning to MARJET the job of producing greater speeds by the extension of high thrust is shown by curve $B$ in Fig. 9.

The procedure for determining the optimum MARJET-hydrofoil design for high-speed cruise requires the determina-

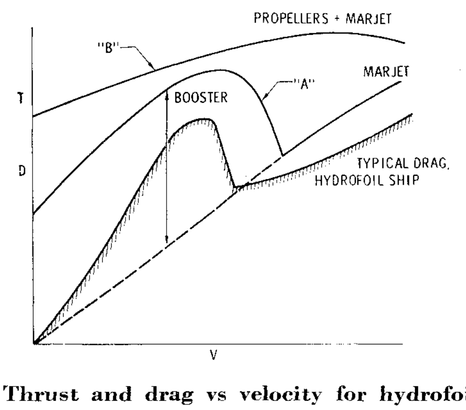


**Fig. 9 Thrust and drag vs velocity for hydrofoil craft.**

**Table 1 Effective thrust**

| | Case I | Case II |
|---|---|---|
| Total shaft horsepower(shp) | 120,000 | 120,000 |
| shp to MARJET | 120,000 | 40,000 |
| Compression ratio | 6.6 | 6.6 |
| Airflow, $Q_A$, ft³/sec | 11,000 | 3,700 |
| Base drag credit, lb | 40,000 | 40,000 |
| Change in MARJET effective thrust, $\Delta TV_0/q_0Q_A$ | 0.028 | 0.080 |

tion of the basic performance (Fig. 5) for the particular speeds (or speed range) adjusted to a given draft condition. Then the external drag components can be estimated for a number of possible power supply, air-to-water ratio, and geometrical parameters. From these estimates, the specific design charts similar to Fig. 8 can be constructed. Approximate best-design areas will be immediately apparent on the basis of the net efficiency lines passing through the origin of the plot. (Application of the appropriate air supply cycle efficiency factors may shift the optimum points slightly, since they are a function of the pressure ratio.)

The preceding procedure will lead to optimum MARJET-hydrofoil design, but the "efficiencies" are misleading since all of the MARJET associated drag is charged against the internal thrust. Although there is some base drag associated with (and charged to) MARJET-hydrofoil design, this item (base drag) is usually considered as a part of the lifting system drag. Thus, for comparative efficiencies, the base drag of the equivalent conventional hydrofoil should be added as a credit to the net MARJET thrust. This is a substantial item as may be seen in Table 1 for a 500-ton hydrofoil ship at 80 knots.

The effective MARJET performance for the two cases is obtained by adding the respective increment to the net thrust coefficient in Fig. 8. The improvement in net efficiency of the MARJET-hydrofoil configuration is shown by the increase in slope of the line from the origin tangent to the performance curve.

The over-all installed efficiency, thrust horsepower/shaft horsepower, depends upon the basic compressor efficiency and basic cycle efficiency

$$\eta_{\text{installed}} = \eta \times \eta_{\text{compressor}} \times \eta_{\text{cycle}}$$

**Table 2 Installed efficiency**

| | Case I | Case II |
|---|---|---|
| $\eta_{\text{MARJET-hydrofoil}}$ | 0.65 | 0.88 |
| $\eta_{\text{compressor}}$ | 0.85 | 0.85 |
| $\eta_{\text{cycle}}$ | | |
| (0) single-stage | 0.76 | 0.76 |
| (1) two-stage with intercooling | 0.87 | 0.87 |
| $\eta_{\text{installed (0)}}$ | 0.42 | 0.57 |
| $\eta_{\text{installed (1)}}$ | 0.48 | 0.65 |

As indicated in Table 2 the most efficient application of MARJET to the hydrofoil ship is in the role of a booster. Even with single-stage compressors, the installed efficiency of MARJET compares favorably with the predicted performance of high-speed propeller-driven configurations. The proportion of total power assigned to MARJET will depend upon particular design configuration studies. It is anticipated that the ideal MARJET share will range from $\frac{1}{3}$ (as in the sample case) to $\frac{1}{2}$ of the total power for ships with supercavitating foils. In such applications the MARJET hydrofoil as a booster will substantially relieve the structural and power transmission problems associated with increasing size and speed of hydrofoil ships.

Since the MARJET does not require highly stressed machinery in the struts and foils, its system reliability can be very high. Thus hydrofoil ship operations that require continuous high power and long service life could profit from the use of MARJET as the prime propulsive means, even though the efficiency might be less than that currently predicted for other propulsion systems.

## References

[1] "MARJET feasibility study 500-ton hydrofoil ship—final report," Martin Co., Rept. ER 12392 (April 1962).

[2] "MARJET design data development 500-ton hydrofoil ship—final report," Martin Co., Rept. ER 13298 (April 1964).

[3] Mottard, E., Jr. and Shoemaker, C. J., "Preliminary investigation of an underwater ramjet powered by compressed air," NASA TN D-991 (December 1961).

[4] Doyle, J. P., "Study of propulsion transmission systems for a 500-ton 80-knot hydrofoil ship," Gibbs and Cox, Inc., Rept. M62-19 (November 1962).